

Cite this: *Nanoscale*, 2011, **3**, 4859

www.rsc.org/nanoscale

PAPER

## Functional characterization of a supramolecular affinity switch at the single molecule level

Volker Walhorn,<sup>a</sup> Christian Schäfer,<sup>bc</sup> Tobias Schröder,<sup>b</sup> Jochen Mattay<sup>b</sup> and Dario Anselmetti<sup>\*,a</sup>

Received 22nd July 2011, Accepted 13th September 2011

DOI: 10.1039/c1nr10912j

Surface-immobilized and switchable resorcin[4]arene receptor molecules were quantitatively investigated with atomic force microscopy (AFM) and AFM-single molecule force spectroscopy (AFM-SMFS). The *upper rim* of the supramolecular receptor cavities was modified with two photodimerizable anthracene moieties. The molecular constitution can be externally switched and controlled by exposure to ultraviolet (UV) light and heat. The topography as well as the complexation affinity against small ammonium guest ions of the two isomers were investigated at the single molecule level. Our results demonstrate the feasibility to externally control the supramolecular receptor's affinity and simultaneously quantify and associate these binding properties with the structural change of the resorcin[4]arenes structure on the basis of the measured molecule corrugation height.

### Introduction

The control of nanoscopic functional units like molecular motors<sup>1,2</sup> is of great interest for anticipated nanomachines or nanotechnological applications. Moreover, the rational design and directed synthesis of supramolecules, which can mimic the function of biomolecules for distinct biomedical and technical applications, is a fascinating and timely issue. It is hoped that, with this reverse engineering approach, artificial and robust molecular motors and synthetic machines can be realized. Since nanomachines rely on cyclic operation and external control, repetitive and reproducible transition between at least two different molecular states—*e.g.* by the conformational transition (switching) between two structural isomers—is mandatory. As external control mechanism and transition stimulus, the interaction of molecules with light, electric, chemical or mechanical potentials is known.<sup>3–7</sup> External activation *via* electronic excitation, energy transfer, and/or ionic transport by light harvesting complexes or energy up conversion in photosynthesis are common concepts in nature. Fundamental for all these processes is the ability to convert electromagnetic energy into conformational changes where specific and non-covalent bonds can be formed and released due to affinity changes.

Pioneering work, where supramolecular receptors were structurally investigated with scanning probe microscopy (SPM)<sup>8–11</sup>

and functionally characterized by AFM-SMFS,<sup>12–26</sup> was published over the last few years. Here, we report on a combined structural and functional single molecule analysis of a supramolecular receptor molecule that was modified with two anthracene groups at the *upper rim* of the resorcin[4]arene, and whose structural conformation can be switched externally by UV-illumination or heat. Since the photodimerization process between the two anthracene groups blocks the entrance of resorcin[4]arene, the affinity properties against guest cation complexation of this photochemical system can be reversibly switched and cycled between an open and a closed isomer, which was already investigated qualitatively by AFM-SMFS experiments.<sup>15</sup> In this paper, the structural and functional changes of this goblet shaped resorcin[4]arene receptor were quantitatively investigated by AFM (Fig. 1) in dynamic nanomechanical single molecule experiments with piconewton (pN) force sensitivity. Topographic variations were monitored by AFM with sub-nanometre resolution and could be associated for the first time with the functional modulation of the assigned binding affinity. Our experiments allowed therefore imaging, addressing, manipulating, and probing of single supramolecules, thus representing a further step towards control and regulation of an artificial receptor in the framework of reverse engineering and biomimetics.

### Materials and methods

#### Sample and probe preparation

Resorcin[4]arenes were synthesized according to a previously published procedure.<sup>27</sup> The receptor's *lower rim* was modified with four dialkyl sulfide chains for surface adsorption, while two photodimerizable anthracene moieties were attached at the *upper*

<sup>a</sup>Experimental Biophysics and Applied Nanoscience, Department of Physics, Bielefeld University, Universitätsstraße 25, 33615 Bielefeld, Germany. E-mail: dario.anselmetti@physik.uni-bielefeld.de; Fax: +49 521 106 2959; Tel: +49 521 106 6870

<sup>b</sup>Organic Chemistry I, Department of Chemistry, Bielefeld University, Universitätsstraße 25, 33615 Bielefeld, Germany

<sup>c</sup>Dipartimento di Chimica "G. Ciamician", Università di Bologna, Via F. Selmi 2, 40126 Bologna, Italy

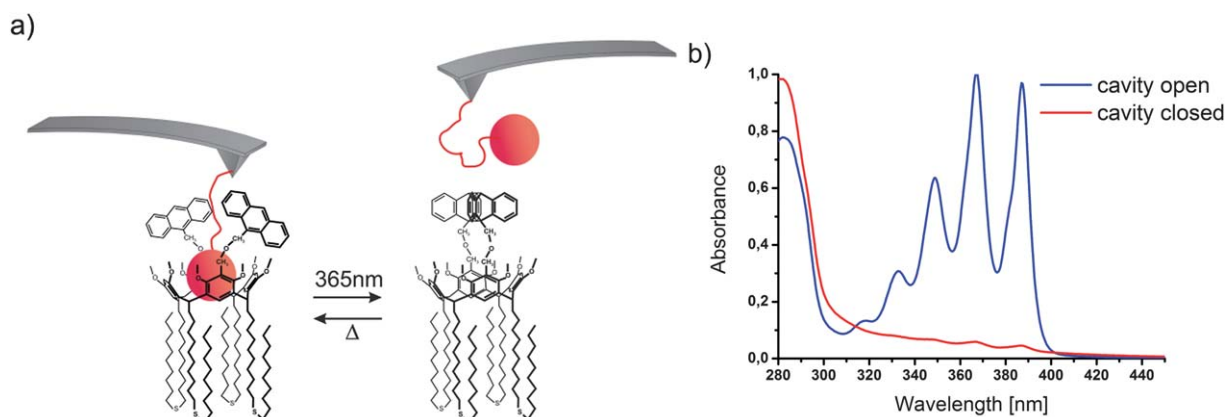


**Fig. 1** (a) Schematic of switchable resorcin[4]arene investigated by AFM SMFS. (b) UV absorption spectra of the resorcin[4]arene receptor. The observed peaks for the open isomer are characteristic for the anthracene moieties.

*rim*. A diluted monolayer of the resorcin[4]arene receptors was self-assembled on template-stripped-gold (TSG) substrates<sup>28,29</sup> for AFM topographical surface characterization and on commercially available gold coated glass slides (Arrandee, Werther, Germany) for AFM-SMFS binding studies, respectively. Briefly, the substrates are incubated with receptor molecules and di-*n*-decyl sulfide solubilized with millimolar concentration in a ratio of 1 : 200 in chloroform–ethanol (1 : 1) and heated to 60 °C for at least 16 hours. After cooling down to room temperature within 2 hours, the substrates were extensively rinsed with chloroform to remove excess physisorbed material. For AFM-SMFS binding studies the guest ions (2-mercaptoethylamine (A) and 6-mercaptohexyl-*N,N,N*-trimethyl ammonium (TMA)) are coupled covalently *via* a flexible poly(ethyleneglycol) (PEG) linker to an AFM-Sensor, allowing steric flexibility, thus facilitating the formation of supramolecular guest–host complexes. In brief, Si<sub>3</sub>N<sub>4</sub>-cantilevers (MSCT, Bruker, Santa Barbara, CA, USA) were dipped in concentrated nitric acid for activation and incubated with a solution of 2% 3-aminopropyltriethylsilane (APTES, Sigma-Aldrich) in dry toluene for 2 hours at ambient temperature. After silanization, the cantilevers were washed with toluene and incubated with 1 mM succinimidyl valerate-poly(ethyleneglycol)-maleimide (*M<sub>w</sub>* 3400, Laysan Bio) in water for 90 min. The cantilevers were washed with water and functionalized by incubating them overnight at room temperature with a 1 millimolar ethanolic solution of the solubilized guest molecules 6-mercaptohexyl-*N,N,N*-trimethyl ammonium chloride and 2-mercaptoethylamine. Modified tips could be stored at 4 °C and remained usable for at least one week. Prior to use in experiment, the cantilevers were washed with ethanol.

### Affinity switching

The switching from closed to open isomers was performed by heating the sample to 60 °C for 2 h in ethanol. Closing the cavity was achieved by irradiation for 20 min with a UV hand lamp (3UV, Ultraviolet Products, Upland CA, USA) at 365 nm. In topographic measurements the sample was directly illuminated in the AFM, whereas it was dismantled from the AFM and immersed in oxygen-free ethanol for the AFM binding studies.

Prior to irradiation, the ethanol was degassed by bubbling nitrogen through the solution for 30 minutes.

### Single molecule force spectroscopy

SMFS experiments were performed with a custom-made AFM system consisting of a home-built AFM head and a dedicated control and data acquisition electronics (ADwin Gold, Jäger Messtechnik, Lorsch, Germany).<sup>30</sup> AFM cantilever spring constants were calibrated *via* the thermal fluctuation method<sup>31</sup> with an absolute uncertainty of approximately 10%; obtained values were in the range from 14.2 to 21.9 pN nm<sup>-1</sup>. The modified probes were repeatedly approached to and retracted from the surface at a variable but constant velocity in the range of 100–5000 s<sup>-1</sup>. Molecular dissociation or rupture events were identified by plotting the cantilever force response *versus* the *z*-piezo position. According to the Kramers–Bell–Evans (KBE) theory, the measured force *F* depends only on the extension *s* of all elastic components of the complex (receptor, ligand, linker and cantilever). Therefore one can define a function *F*(*s*) (referred to as master curve) that every measured force extension curve should lie on regardless of pulling speed or linker properties.<sup>32</sup> Consequently, the non-linear elastic stretching of the PEG linker preceding the bond rupture bears the molecular elasticity and served as criterion to discriminate single binding events from unspecific adhesion. As molecular dissociation is of stochastic nature, rupture forces from many unbinding events (typical 400) are plotted in a force histogram. The peak of the resulting force distribution can be approximated by a Gaussian distribution and is commonly referred to as the most probable dissociation force *F*\*. Dissociation forces depend on the temporal evolution of an external applied force and therefore directly relate to the molecular loading rate *r*, which is defined as the product of the molecular elasticity and the retract velocity. In dynamic force spectroscopy mode, the pulling velocity is now experimentally varied and the measured dissociation forces *F*\* are plotted semi-logarithmically *versus* the loading-rate. In thermally driven single molecule dissociation theory under non-equilibrium conditions (KBE-model), loading rates *r* and most probable dissociation forces *F*\* are logarithmically related and can be fitted corresponding to the formula given by Strunz *et al.*:<sup>33</sup>

$$F^* = \frac{k_B T}{x_\beta} \ln \left( \frac{x_\beta r}{k_B T k_{\text{off}}^0} \right),$$

where  $k_B T = 4.11$  pN nm,  $x_\beta$  and  $k_{\text{off}}^0$  denote the Boltzmann factor at room temperature (298 K), molecular reaction length and reaction off-rate constant at zero load, respectively. The slope of the linear fit correlates with the width of the last binding potential barrier along the reaction coordinate of the system (activation energy), yielding  $x_\beta$ . Upon extrapolation of the linear fit to zero external force, the thermal off-rate constant for the complex can be obtained. Although this analysis method has proven its validity and practicability in the last decade, it suffers from smaller, model-inherent inconsistencies.<sup>34</sup> Alternatively, the heterogeneous-bond-model (HB-model)—an extension to the KBE-theory—was developed, where stochastic variations of the local molecular environment were considered, resulting in a more consistent theoretical picture.<sup>35</sup> However, this makes a statistically more elaborate experimental dataset necessary, and leads to a dispersion of the reaction length  $x_\beta$  giving a mean  $\bar{x}_\beta$  with a variance of  $\sigma^2$ . Estimating the most probable set of parameters

$\mu = \left( k_{\text{off}}^0, \frac{x_\beta}{k_B T}, \sigma \right)$  maximizes the likelihood function  $L(\mu)$ :

$$L(\mu) = \prod_{i=1}^N p(f_i | \mu, v, F(s), f_{\text{min}}),$$

where  $f_i$  denotes a set of dissociation forces,  $v$  the pulling velocity and  $f_{\text{min}}$  the minimum detectable force. For a more detailed and comprehensive description the interested reader may refer to the literature.<sup>36,37</sup>

## Molecular surface topography

AFM topographs were acquired with a Multimode AFM (Veeco, Santa Barbara CA, USA) in tapping mode of operation under ambient conditions using sharp silicon probes (NCL Nanosensors, Neuchatel, Switzerland). To unequivocally determine topographic changes of single supramolecular receptors due to photodimerization of anthracene groups, the very same region of interest was scanned at least three times before and after UV-illumination, respectively. Successive cross-sections of the two sets were superimposed to evaluate and quantify the average height.

## Results and discussion

### Topography

Switchable resorcin[4]arenes were immobilized on TSG substrates as described and imaged under ambient conditions at room temperature. Due to the extremely low surface roughness, TSG substrates are ideally suited for high resolution topographic imaging. Nevertheless, every substrate was characterized prior to use and only substrates with a mean roughness lower than 0.2 nm (RMS, on 1  $\mu\text{m}^2$ ) were used for receptor immobilization. This selective process guaranteed clear and unequivocal identification of the individual receptor molecules as small surface protrusions (Fig. 2a). For better analysis, a region of interest was defined and identically cut out from several consecutive scans before and after UV illumination (Fig. 2b). The extracted cross-sections

were superimposed to estimate the change of the apparent molecule height caused by the conformational transition induced by UV-irradiation (Fig. 2c). As can clearly be discerned from this image, a reproducible and significant topography change of  $182 \pm 42$  pm can be identified, where the larger corrugation amplitude can be associated with resorcin[4]arenes in the (closed) constitution. We analyzed 18 molecules from several samples and determined a mean increase of  $221 \pm 43$  pm. Taking the root-mean-square surface roughness as an estimate for the (topographical) “noise” we got a signal-to-noise ratio better than 4. It is very likely that this change in the apparent molecule height can be associated with the photodimerization of the anthracene groups as anthracene dimers are supposed to withstand the probe impact much better than the monomers. This difference in the apparent molecule height of the isomers can be allocated to both the different molecular topography as well as to the different contributions from the local nanometric force response between AFM tip and receptor. It is very likely that the photocyclized resorcin[4]arene complex can withstand the mechanical AFM probe impact much better than the macrocycle in the open structure. Comparing the length of the shorter axis of a single anthracene molecule of 280 pm<sup>38</sup> to the measured increment confirmed the validity of the results. It is worth noting that photodimerization of anthracene in ambient conditions shows a low fatigue resistance as the anthracene dimerization competes with several other irreversible photochemical reactions like *e.g.* oxidation.<sup>39</sup> Due to experimental constraints the UV-irradiation was done in ambient conditions. Consequently the photoreaction yield was rather small.

### Single molecule force spectroscopy

Affinity-switchable resorcin[4]arenes were self-assembled on gold coated glass slides as described. Single molecule affinity studies of these receptors against A (ammonium) and TMA (trimethylammonium) guest cations were performed in ethanol at room temperature. Several series of force spectroscopy experiments were done. For UV-illumination, the samples were dismounted and immersed in degassed ethanol. A set of force extension curves was acquired for each guest cation at retract velocities in the range of 100–5000 nm s<sup>-1</sup> yielding loading rates varying from 700 to 80 000 pN s<sup>-1</sup>. According to the KBE theory, the experimentally most probable rupture forces were estimated and plotted *versus* the loading rate (Fig. 3). Fitting of the different datasets yielded an interaction length of  $x_\beta = 0.265 \pm 0.059$  nm and a thermal off-rate constant of  $k_{\text{off}}^0 = 0.54 \pm 0.77$  s<sup>-1</sup> for the guest cation A, and  $x_\beta = 0.422 \pm 0.082$  nm and  $k_{\text{off}}^0 = 0.09 \pm 0.15$  s<sup>-1</sup> for the guest TMA residue, respectively. This is equivalent with average bond lifetimes ( $k_{\text{off}}^0 = \tau^{-1}$ ) of  $\tau = 1.9$  s (for A) and  $\tau = 11.1$  s (for TMA), respectively. Alternatively, upon applying the HB-model to our results yielded  $x_\beta = 0.148 \pm 0.006$  nm and  $k_{\text{off}}^0 = 0.42 \pm 0.05$  s<sup>-1</sup> for guest cation A, and  $x_\beta = 0.324 \pm 0.016$  nm and  $k_{\text{off}}^0 = 0.22 \pm 0.08$  s<sup>-1</sup> for the TMA residue, respectively, corresponding to average lifetimes of  $\tau = 2.3$  s (A) and  $\tau = 4.5$  s (TMA). Although the estimated figures of both theoretical models somewhat differ, the overall values consistently reproduce, also reflecting the correct relative gradation. Interestingly, both models consistently state longer bond lifetimes and larger interaction lengths for the larger TMA guest

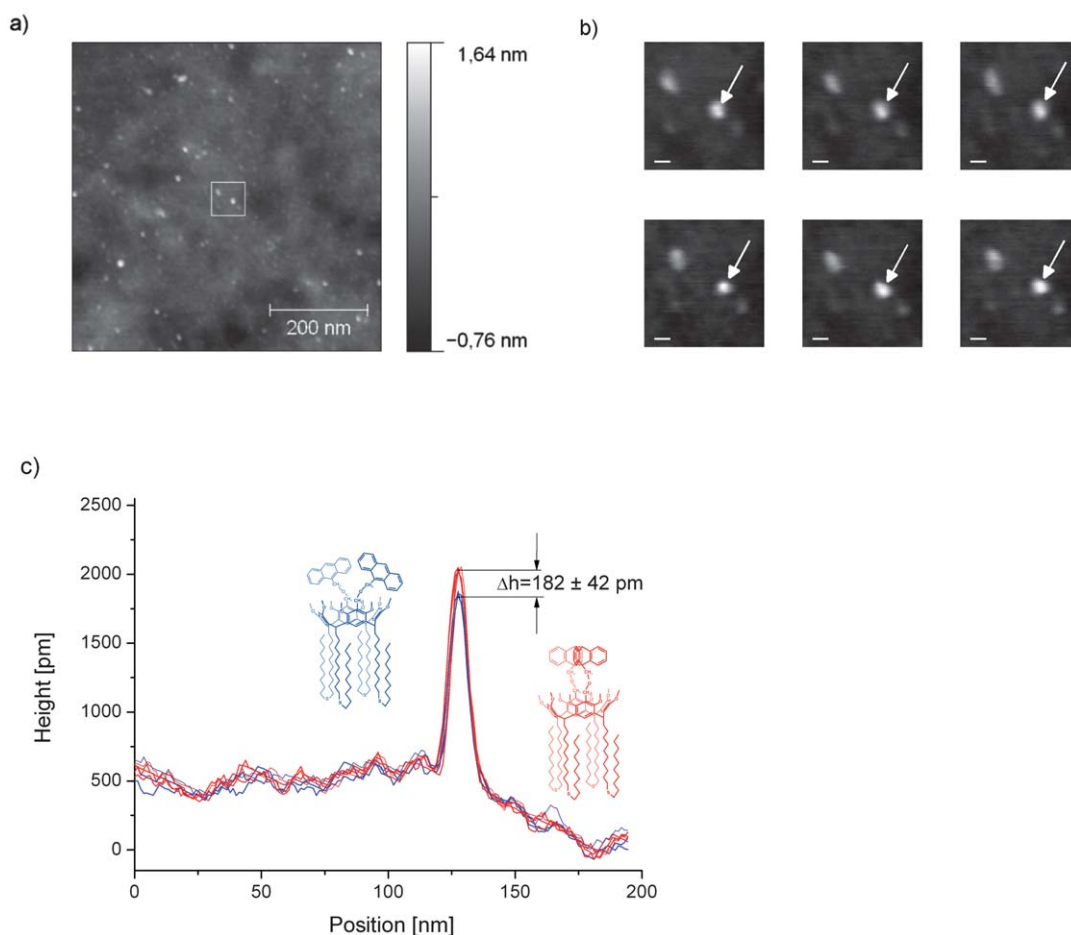


**Fig. 2** (a) AFM topography of single immobilized anthracene modified resorcin[4]arenes on a TSG substrate embedded in a monolayer of di-*n*-decyl sulfide. The very same region of interest (box) is cut out from successive AFM scans to extract cross-sections of single molecules. (b) Whereas the three top row images were taken before UV exposure, the three bottom row images were measured after UV-exposure. The scale bar indicates 20 nm. (c) Cross-sections of the marked molecule (arrows in b) are superimposed to estimate the apparent molecule height, yielding a larger corrugation amplitude that can be associated with resorcin[4]arenes in the dimerized (closed) constitution (red curves, after UV exposure) in contrast to receptors in the open constitution (blue curves, before UV exposure).

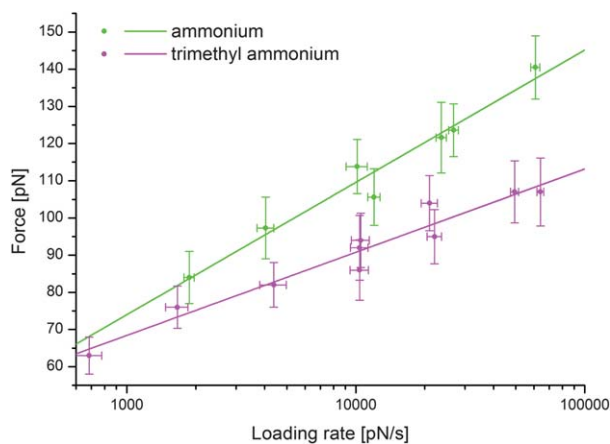


**Fig. 3** SMFS, most probable dissociation forces plotted semi-logarithmically against the corresponding loading rates, for binding of the ammonium and trimethyl ammonium residues to the resorcin[4]arene.

ligand, indicating a more intimate and tight complexation with the probed rim-modified resorcin[4]arene, in full consistency with the results of an earlier experiment with the unmodified compound.<sup>15</sup> In order to evaluate the overall binding affinity, the association rate constant  $k_{\text{on}}^0$  can be assumed not to show strong variations, such as that the dissociation constant of equilibrium  $K_{\text{D}} = k_{\text{off}}^0/k_{\text{on}}^0$  is mainly dominated by  $k_{\text{off}}^0$ .<sup>40</sup> On assuming a diffusion limited association rate constant of  $k_{\text{on}}^0 = 5 \text{ M}^{-1} \text{ s}^{-1}$ ,<sup>40,41</sup> the Gibbs free energy  $\Delta G = RT \ln K_{\text{D}}$  of the complexation reaction can be estimated. Depending on the used theoretical model, we derived binding energies of  $-30.0/-30.7 \text{ (kJ mol}^{-1}\text{)}$  (KBE-model/HB-model) for A and  $-34.5/-32.3 \text{ (kJ mol}^{-1}\text{)}$  for TMA, respectively, further supporting the tighter complexation of the TMA ligand compared to A, in excellent agreement with the results of Eckel *et al.*<sup>15</sup> Furthermore, the results of both models are fully consistent with calorimetric data obtained from comparable guest–host complexes like cyclodextrins<sup>12</sup> and water-soluble cavitands.<sup>42</sup>

The fundamental of the KBE- and HB-models is the reaction-rate theory formulated by Kramers.<sup>43</sup> The KBE-model has

proven its validity as a solid found to analyze SMFS data for thermal non-equilibrium conditions over the last decade. Although in some supramolecular systems like cyclodextrins,<sup>14</sup> hydrogen-bonded pyrimidine systems<sup>19,18</sup> or  $\pi$ - $\pi$ -bridged systems,<sup>21,22</sup> fast complexation phenomena with quasi-equilibrium conditions could be observed, the host-guest-binding kinetics of most supramolecular systems can be quantitatively described within the framework of non-equilibrium conditions and the KBE-model.<sup>15-17,19,23,25,26,44,45</sup> Nevertheless, there are some deficiencies in the KBE-model, making it necessary to extend the current formalism. The HB-model accounts for the local statistical fluctuations that the molecular environment is subjected to, like variations in the ionic strength, pH, molecular structure or the direction of the externally applied force. Overall, the results of the HB-model are comparable to those gained with

the KBE-model. However, it is known that the HB-model favorably approximates the distribution of the dissociation forces, in a much better and coherent way than the KBE-model, especially in the high force regime.<sup>36</sup>

For verification of the specificity of the guest-host interaction, the switchability of the receptor affinity and as a control experiment, we performed five consecutive series of force spectroscopy experiments between the switchable resorcin[4]arene and its cationic guest ligand TMA as visualized in the corresponding force histograms (Fig. 4 a-e). The first set of series was measured on the open receptor immediately after sample preparation (Fig. 4a). Here, we derived a most probable dissociation force of 84 pN at an experimental velocity of 500 nm s<sup>-1</sup>. Integrating the distribution gives an overall binding probability of 4.4%. This considerably small absolute value

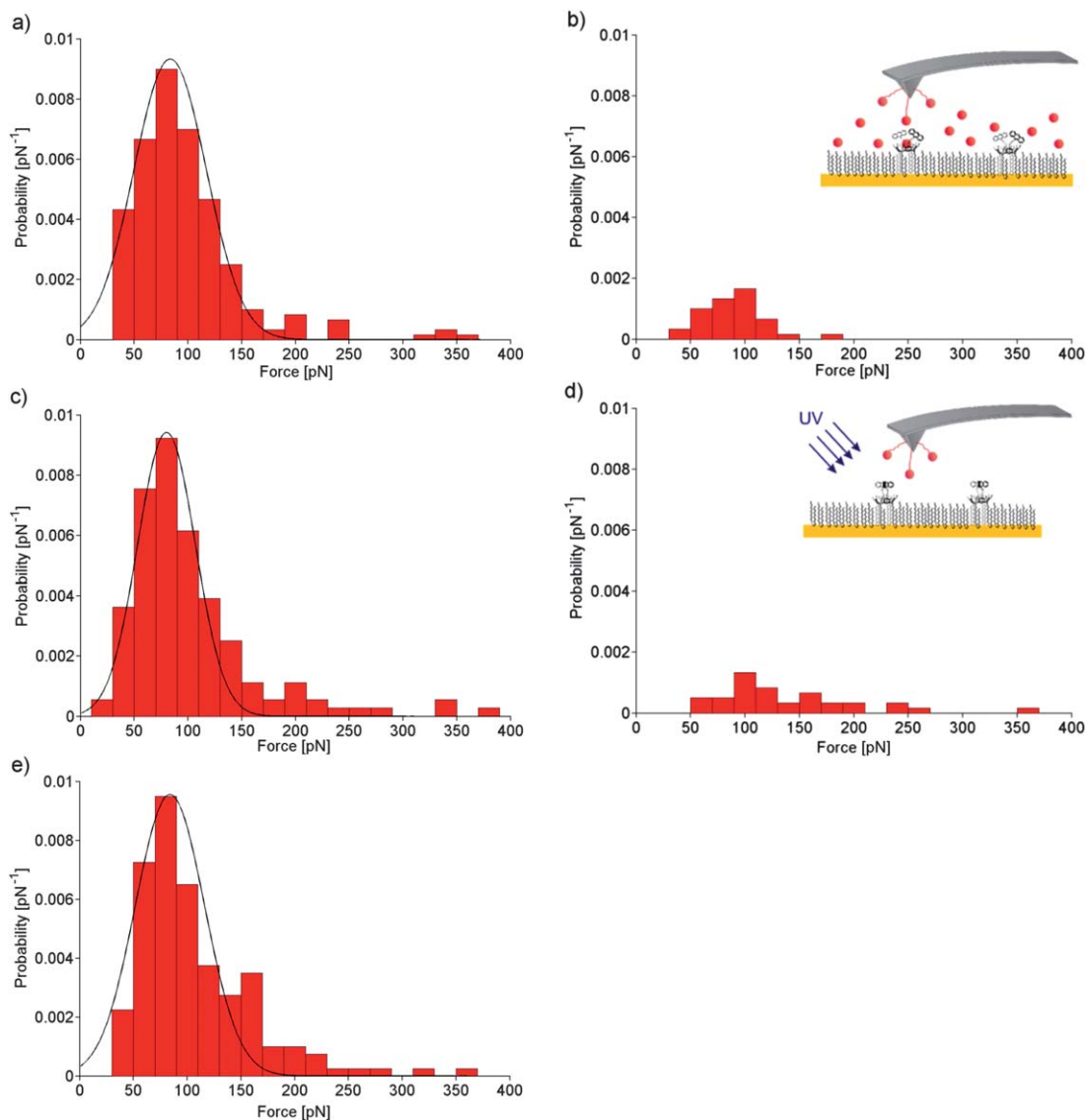


**Fig. 4** Single-molecule force spectroscopy experiments with switchable resorcin[4]arene. (a) Initial series after sample preparation. (b) Series after irradiating the sample surface at 365 nm for 20 min in degassed ethanol. (c) Series after reactivating the sample by heating to 60 °C for 2 h. (d) Series of competition experiments, performed in ethanolic solution saturated with free tetramethyl ammonium chloride. (e) Reactivated surface after extensive rinsing with ethanol. All experiments were performed with the same tip and sample at a retract velocity of 500 nm s<sup>-1</sup>. For each force histogram in (a) to (e) typically more than three hundred rupture events were statistically analyzed.

reflects the fact that we worked with a very low surface coverage of resorcin[4]arenes (see also Fig. 2a and preparation protocol). Although such a low surface coverage decreases the binding probability and makes AFM force spectroscopy experiments more tedious, on the other hand, it helps to reduce unwanted multiple binding events as well as binding cross-talk due to anthracene dimerization between different receptors at the surface, and last but not least, helps to spatially resolve and discriminate individual receptor molecules by AFM imaging. Upon adding free TMA ligand (tetramethyl ammonium chloride) to the solution, this leads to a blockade of the receptors resulting in a significant and remarkable decrease of the binding probability to 0.6% (Fig. 4b). The original surface binding activity could then be restored after washing the sample extensively with ethanol. There, the dissociation force histogram as well as the most probable dissociation force corresponds again to the initial series (Fig. 4c). Next, the sample was irradiated with UV light in oxygen-free ethanol and a new force spectroscopy series was recorded. The corresponding dissociation force histogram again shows an apparent decrease of the overall binding probability to 0.4% which is due to the dimerization of the anthracene moieties blocking the receptor cavity (Fig. 4d). Subsequent heating for 2 h at 60 °C in degassed ethanol reactivates the surface and restores the binding probability again to the initial level (Fig. 4e). The remarkable impact of the competing free ions and the formation of the anthracene dimers serve as unequivocal evidence for the specificity of the molecular recognition between the host and guest and the switchability of the receptor's affinity as measured in single molecule force spectroscopy (SMFS).

## Conclusion

In summary, we present the quantitative investigation of a supramolecular complexation reaction between a photoactive anthracene modified resorcin[4]arene receptor cavity and two cationic ammonium guest ligands at the single molecule level. Our experiments confirm that the receptor can be reversibly and reproducibly toggled between two different structural isomers by means of UV irradiation (open → closed cavity) and heat (closed → open cavity). SMFS experiments demonstrated the feasibility to reversibly affinity switch the surface-immobilized supramolecular receptors, to measure reaction off-rate constants, binding lengths as well as to estimate equilibrium constants and binding energies. The different receptor structures were identified by their affinity against ammonium cations: whereas the open isomer shows a high affinity to ammonium and trimethyl ammonium ligands, the closed isomer exhibits almost none. Additionally, we could prove and quantify the increase of the apparent molecule corrugation height due to photodimerization of the anthracene moieties by AFM under ambient conditions.

Since anthracene modified resorcin[4]arenes, functionally immobilized on metallic surfaces, display rather robust binding properties, they might serve as model for various future applications using self-assembled monolayers. There, locally structured functional surfaces (e.g. arrays) can be prepared by UV writing and erasing procedures to recognize and bind molecules.

## Acknowledgements

The authors acknowledge support from the Collaborative Research Center SFB 613 from the Deutsche Forschungsgemeinschaft (DFG).

## References

- 1 V. Balzani, A. Gredi and M. Venturi, *Molecular Devices and Machines*, Wiley-VCH, 2008.
- 2 *Molecular Motors*, ed. M. Schliwa, Wiley-VCH, 2002.
- 3 V. Bermudez, N. Capron, T. Gase, G. Gatti, F. Kajzar, D. A. Leigh, F. Zerbetto and S. Zhang, *Nature*, 2000, **406**, 608.
- 4 F. Moresco, G. Meyer, K. H. Rieder, H. Tang, A. Gourdon and C. Joachim, *Phys. Rev. Lett.*, 2001, **86**, 672.
- 5 R. A. Bissell, E. Corodva, A. E. Kaifer and J. F. Stoddart, *Nature*, 1994, **369**, 133.
- 6 J. Walz, K. Ulrich, H. Port, H. Wolf, J. Wonner and F. Effenberger, *Chem. Phys. Lett.*, 1993, **213**, 321.
- 7 I. Willner, *Acc. Chem. Res.*, 1997, **30**, 347.
- 8 E. Menozzi, R. Pinalli, E. A. Speets, B. J. Ravoo, E. Dalcanale and D. N. Reinhoudt, *Chem.–Eur. J.*, 2004, **10**, 2199.
- 9 G.-B. Pan, J.-H. Bu, D. Wang, J.-M. Liu, L.-J. Wan, Q.-Y. Zheng and C.-L. Bai, *J. Phys. Chem. B*, 2003, **107**, 13111.
- 10 G.-B. Pan, L.-J. Wan, Q.-Y. Zheng, C.-L. Bai and K. Itaya, *Chem. Phys. Lett.*, 2002, **359**, 83.
- 11 M. Namba, M. Sugawara, P. Buehlmann and Y. Umezawa, *Langmuir*, 1995, **11**, 635.
- 12 T. Auletta, M. R. de Jong, A. Mulder, F. C. J. M. van Veggel, J. Huskens, D. N. Reinhoudt, S. Zou, S. Zapotoczny, H. Schönherr, G. J. Vancso and L. Kuipers, *J. Am. Chem. Soc.*, 2004, **126**, 1577.
- 13 H. Schönherr, M. W. J. Beulen, J. Bügler, J. Huskens, F. C. J. M. van Veggel, D. N. Reinhoudt and G. J. Vancso, *J. Am. Chem. Soc.*, 2000, **122**, 4963.
- 14 S. Zapotoczny, T. Auletta, M. R. de Jong, H. Schönherr, J. Huskens, F. C. J. M. van Veggel, D. N. Reinhoudt and G. J. Vancso, *Langmuir*, 2002, **18**, 6988.
- 15 R. Eckel, R. Ros, B. Decker, J. Mattay and D. Anselmetti, *Angew. Chem., Int. Ed.*, 2005, **44**, 484.
- 16 C. Schäfer, R. Eckel, R. Ros, J. Mattay and D. Anselmetti, *J. Am. Chem. Soc.*, 2007, **129**, 1488.
- 17 D. Anselmetti, F. W. Bartels, A. Becker, B. Decker, R. Eckel, M. McIntosh, J. Mattay, P. Plattner, R. Ros, C. Schafer and N. Sewald, *Langmuir*, 2008, **24**, 1365.
- 18 S. Zou, H. Schönherr and G. J. Vancso, *Angew. Chem., Int. Ed.*, 2005, **44**, 956.
- 19 S. Zou, H. Schönherr and G. J. Vancso, *J. Am. Chem. Soc.*, 2005, **127**, 11230.
- 20 A. Embrechts, H. Schönherr and G. J. Vancso, *J. Phys. Chem. B*, 2008, **112**, 7359.
- 21 Y. Zhang, C. Liu, W. Shi, Z. Wang, L. Dai and X. Zhang, *Langmuir*, 2007, **23**, 7911.
- 22 Y. Zhang, Y. Yu, Z. Jiang, H. Xu, Z. Wang, X. Zhang, M. Oda, T. Ishizuka, D. Jiang, L. Chi and H. Fuchs, *Langmuir*, 2009, **25**, 6627.
- 23 F. R. Kersey, W. C. Yount and S. L. Craig, *J. Am. Chem. Soc.*, 2006, **128**, 3886.
- 24 Z. Guan, J. T. Roland, J. Z. Bai, S. X. Ma, T. M. McIntire and M. Nguyen, *J. Am. Chem. Soc.*, 2004, **126**, 2058.
- 25 T. Schröder, T. Geisler, V. Walhorn, B. Schnatwinkel, D. Anselmetti and J. Mattay, *Phys. Chem. Chem. Phys.*, 2010, **12**, 10981.
- 26 M. Janke, Y. Rudzevich, O. Molokanova, T. Metzroth, I. Mey, G. Diezemann, P. E. Marszalek, J. Gauss, V. Böhmer and A. Janshoff, *Nat. Nanotechnol.*, 2009, **4**, 225.
- 27 C. Schäfer and J. Mattay, *Photochem. Photobiol. Sci.*, 2004, **3**, 331.
- 28 M. Hegner, P. Wagner and G. Semenza, *Surf. Sci.*, 1993, **291**, 39.
- 29 P. Wagner, M. Hegner, H. J. Güntherodt and G. Semenza, *Langmuir*, 1995, **11**, 3867.
- 30 R. Eckel, V. Walhorn, C. Pelargus, J. Martini, T. Nann, A. Anselmetti and R. Ros, *Proc. SPIE–Int. Soc. Opt. Eng.*, 2006, **6092**, 609209.
- 31 J. L. Hutter and J. Bechhoefer, *Rev. Sci. Instrum.*, 1993, **64**, 1868.
- 32 E. Evans and K. Ritchie, *Biophys. J.*, 1997, **72**, 1541.

- 
- 33 T. Strunz, K. Oroszlan, I. Schumakovitch, H. Güntherodt and M. Hegner, *Biophys. J.*, 2000, **79**, 1206.
- 34 M. Raible, M. Evstigneev, P. Reimann, F. W. Bartels and R. Ros, *J. Biotechnol.*, 2004, **112**, 13.
- 35 M. Raible, M. Evstigneev, F. W. Bartels, R. Eckel, M. Nguyen-Duong, R. Merkel, R. Ros, D. Anselmetti and P. Reimann, *Biophys. J.*, 2006, **90**, 3851.
- 36 S. Getfert and P. Reimann, *Phys. Rev. E: Stat., Nonlinear, Soft Matter Phys.*, 2007, **76**, 052901.
- 37 A. Fuhrmann, D. Anselmetti, R. Ros, S. Getfert and P. Reimann, *Phys. Rev. E: Stat., Nonlinear, Soft Matter Phys.*, 2008, **77**, 031912.
- 38 F. R. Ahmed and D. W. J. Cruickshank, *Acta Crystallogr.*, 1952, **5**, 852.
- 39 H. Bouas-Laurent, A. Castellan, J. P. Desvergne and R. Lapouyadec, *Chem. Soc. Rev.*, 2000, **29**, 43.
- 40 F. Schwesinger, R. Ros, T. Strunz, D. Anselmetti, H. J. Güntherodt, A. Honegger, L. Jermutus, L. Tiefenauer and A. Plückthun, *Proc. Natl. Acad. Sci. U. S. A.*, 2000, **97**, 9972.
- 41 M. Schlosshauer and D. Baker, *Protein Sci.*, 2004, **13**, 1660.
- 42 T. Haino, D. M. Rudkevich, A. Shivanyuk, K. Rissanen and J. Rebek, *Chem.–Eur. J.*, 2000, **6**, 3797.
- 43 H. A. Kramers, *Physica*, 1940, **7**, 284.
- 44 C. Schäfer, B. Decker, M. Letzel, F. Novara, R. Eckel, R. Ros, D. Anselmetti and J. Mattay, *Pure Appl. Chem.*, 2006, **78**, 2247.
- 45 *Analytical Methods in Supramolecular Chemistry*, ed. C. Schalley, Wiley-VCH, 2nd edn, 2011, in press.